PFG – Journal of Photogrammetry, Remote Sensing and Geoinformation Science
https://doi.org/10.1007/s41064-024-00284-0

ORIGINAL ARTICLE

Evaluating Sea Level Rise Impacts on the Southeastern Türkiye Coastline: a Coastal Vulnerability Perspective

Fahri Aykut[1] · **Devrim Tezcan**[1]

Received: 30 November 2023 / Accepted: 5 March 2024

Abstract
Coastal areas are inherently sensitive and dynamic, susceptible to natural forces like waves, winds, currents, and tides. Human activities further accelerate coastal changes, while climate change and global sea level rise add to the challenges. Recognizing and safeguarding these coasts, vital for both socioeconomic and environmental reasons, becomes imperative. The objective of this study is to categorize the coasts of the Mersin and İskenderun bays along the southeastern coast of Türkiye based on their vulnerability to natural forces and human-induced factors using the coastal vulnerability index (CVI) method. The study area encompasses approximately 520 km of coastline. The coastal vulnerability analysis reveals that the coastal zone comprises various levels of vulnerability along the total coastline: 24.7% (128 km) is categorized as very high vulnerability, 27.4% (142 km) as high vulnerability, 23.7% (123 km) as moderate vulnerability, and 24.3% (126 km) as low vulnerability. Key parameters influencing vulnerability include coastal slope, land use, and population density. High and very high vulnerability are particularly prominent in coastal plains characterized by gentle slopes, weak geological and geomorphological features, and significant socioeconomic value.

Keywords Climate Change Impacts · Global Sea Level Projections · Mersin · Socio-Economic Vulnerability · Eastern Mediterranean

1 Introduction

Coastal regions play a vital role in human activities, economic activities, and the preservation of coastal ecosystems. It is reported that approximately 37% of the global population resides within 10 km of the coast (OC 2017). Coastal economic activities, including trade, tourism, fisheries, and various industries, constitute a substantial portion of the global economy (WOR 2017; EC Report 2016; Randone et al. 2017). Additionally, coastal areas serve as critical providers of essential marine ecosystem services.

On the other hand, coastal areas are highly vulnerable and dynamic ecosystems, susceptible to rapid changes caused by both human-induced factors and climate-related impacts (De La Cruz 2021). Climate change has many significant impacts on coastal areas, with sea level rise (SLR) being among the major climate change-induced risks of the 21th century for coastal areas (Nicholls and Cazenave 2010).

SLR is primarily driven by global warming which results from increased concentrations of greenhouse gases in the Earth's atmosphere. Additionally, human activities in recent decades have accelerated the warming of the planet and contributed to the rise in sea levels.

The Intergovernmental Panel on Climate Change (IPCC) has projected SLR scenarios for 2100 based on climate mitigation success. Even the best scenario predicts a rise of 0.28–0.55 m, while the worst-case scenario reaches 1 m (IPCC 2014). SLR leads to increased coastal erosion, higher storm surges, and saltwater intrusion into freshwater sources, severely affecting low-lying coastal areas (IPCC 2019). Unpredictable weather events and extreme precipitation further exacerbate these threats. Authorities and coastal planners need a coastal vulnerability assessment to address these threats.

The Mediterranean basin, identified as one of the primary hotspots for climate change, is warming at a rate 20% faster than the global average, according to Med (2020). Compared to other coastal regions worldwide, Mediterranean cities, wetlands, and drylands are projected to suffer the

✉ Devrim Tezcan
dtezcan@metu.edu.tr

[1] Institute of Marine Sciences, Middle East Technical University, Mersin, Turkey

Published online: 19 April 2024

most damage due to SLR in the 21st century (Marcos et al. 2016). The southeastern coastal region of Türkiye, characterized by low-lying areas, deltas, and natural preserves, faces significant risks from global threats such as SLR.

The vulnerability of coastal areas depends on both the physical characteristics of the coast and human activities along the coast. To assess vulnerability, various coastal vulnerability index (CVI) tools have been developed (Gornitz 1990, Gornitz et al. 1997, Thieler and Hammar-Klose 1999, Szlafsztein and Sterr 2007, McLaughlin and Cooper 2010).

The Thieler and Hammar-Klose (1999) model, which is an adapted version of Gornitz (1990), is the most widely used CVI method for assessing coastal vulnerability against SLR. Owing to the widespread availability of satellite data, this method has been employed by researchers globally (Charuka et al. 2023, Mendoza et al. 2023, Kuleli and Bayazıt 2023, Ozsahin et al. 2023, Gaki-Papanastassiou et al. 2010, Addo 2013, Gorokhovich et al. 2014, Kunte et al. 2014, Diez et al. 2007). However, this model only considers the physical attributes of coastal areas, including coastal geomorphology, coastal slope, historical shoreline change, mean tidal change, mean wave height, and the rate of sea level rise.

Similar to the physical factors, socioeconomic factors also have significant impacts on coastal vulnerability (Boruff et al. 2005). Socioeconomic factors encompass all human activities on coastal areas such as infrastructures, settlements, sensitive coastal and marine ecosystems.

Socioeconomic transformations tend to happen more rapidly than physical alterations when considering both physical and socioeconomic aspects of vulnerability (Szlafsztein and Sterr 2007). As an example, population and tourist density are identified as key influencers of coastal vulnerability, particularly in Goa, India, where the escalating population and tourism's crucial economic role intertwine to shape the region's coastal resilience (Kunte et al. 2014).

Another important socioeconomic factor, the land use, provides a more comprehensive representation of the cultural, economic, and environmental values of coastal areas (Maanan et al. 2018). Also, the conservation areas should be included in vulnerability assessments to effectively identify regions with significant ecological and biological importance (Maanan et al. 2018).

The model by Thieler and Hammar-Klose (1999) was adapted in some studies to incorporate socioeconomic parameters into vulnerability assessments (Dada et al. 2024, Charuka et al. 2023). In this adapted approach, both physical and socioeconomic factors contribute equally to the overall assessment. Another methodology, the multi-scale CVI method developed by McLaughlin and Cooper (2010), described the vulnerability as a combination of factors including coastal characteristics (such as geomorphology, coastline type, and elevation), coastal forces (like wave height and tidal range), and socioeconomic elements (including population, cultural heritage, and roads) which together create three sub-indices for the coastal vulnerability index (CVI). This approach divides the CVI into three sub-indices, each with normalized scores that contribute equally to the composite vulnerability assessment, as detailed by McLaughlin and Cooper (2010).

Several studies have evaluated coastal vulnerability in Türkiye, but only a limited number address this specific study area. Kahraman and Sılaydın Aydın and Kahraman (2016) examined the susceptibility of coastal cities in Türkiye to SLR using the CVI method. The findings indicated that Mersin city exhibits a lower level of vulnerability compared to other cities. Kuleli (2010) developed an index specifically tailored to assessing the risk of SLR in coastal zones on a city-by-city basis. This index incorporates physical data along with a range of socioeconomic metrics, including population, settlements, land use, wetlands, contributions to national agricultural production, and tax revenues. A key finding of this study, relevant to the region under consideration, is that the Mediterranean region is identified as being particularly susceptible to land loss due to SLR. In a similar study, Kurt and Li (2020) explored the impacts of sea level changes on the coastlines of Turkey. Utilizing elevation data along with a selection of socioeconomic factors such as population and settlements, their analysis revealed that out of the 28 provinces examined, Adana, Edirne, Izmir, and Samsun are the most susceptible to the spatial changes caused by rising sea levels.

An additional CVI-SLR method that incorporates both physical and human influence parameters was developed by Ozyurt and Ergin (2010). This approach calculates the index using five sub-indices, each representing a different impact of SLR: coastal erosion, flooding due to storm surge, inundation, salt water intrusion to groundwater resources, and salt water intrusion to river and estuaries. Each sub-index is calculated using both physical elements and the impact of human activities. This method has been applied to the Göksu Delta in Türkiye, an area where all five considered impacts of SLR are present. In Göksu Delta, located in this study area, the researchers utilized 12 physical and 7 human influence parameters, with each parameter potentially contributing more than one sub-index. This method uniquely emphasizes the most vulnerable areas by directly correlating both numerical and qualitative data with specific physical effects. However, a challenge with this method is the difficulty in obtaining high-resolution data at all locations.

Simav et al. (2013) carried out an extensive analysis to evaluate the vulnerability of the Çukurova Delta to projected inundation. They utilized multi-mission satellite altimetry sea level anomaly and significant wave height data,

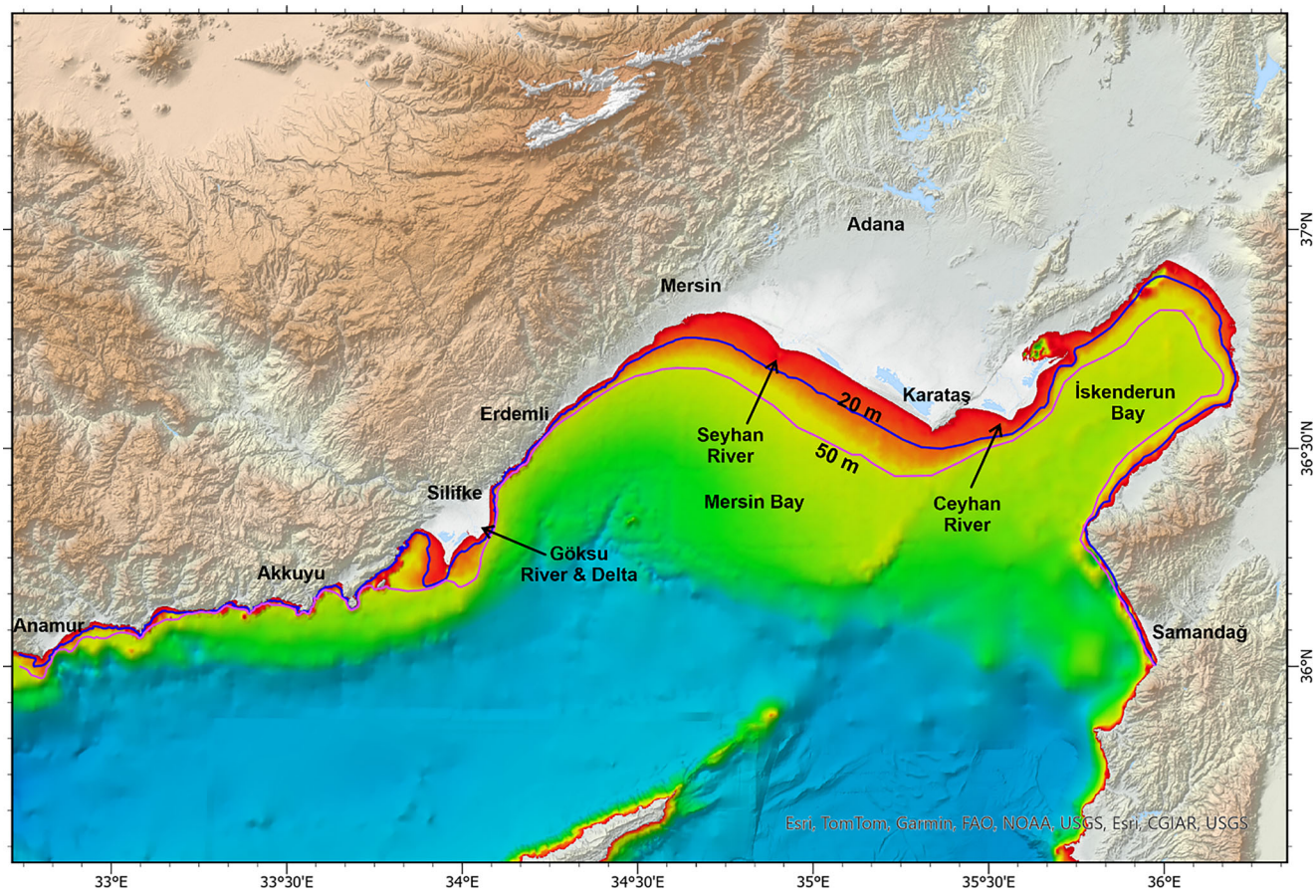

Fig. 1 Overview of the study area. This map provides a visual representation of both land relief and underwater bathymetry, using a *color gradient* from *red* for shallow waters to *blue* for deeper regions. The depth contours at 20 m and 50 m are marked by *blue* and *pink lines*, respectively

aiming to enhance wetland conservation and management efforts in the Çukurova Delta. Their findings explicitly show that the maximum anticipated flooding level by the year 2100 could reach up to 6.7 m, underscoring the importance of conducting vulnerability assessments for this region.

Aykut (2021) conducted an initial assessment of coastal vulnerability in the southeastern region of Turkey. This study involved a comparison and application of five distinct coastal vulnerability index methods to this specific area. Aykut (2021) noted that incorporating socioeconomic parameters could significantly alter the assessment outcomes.

The coastal region in this study holds significant economic value due to its coastal tourism, agriculture, numerous industrial zones, and thermal power plants. It is also notable as the site of Türkiye's first nuclear power plant, which is currently under construction. At the same time, the region has experienced a substantial increase in population. This growth has been driven by the arrival of immigrants and refugees from countries affected by war and political instability, as well as by people displaced by the earthquakes in February 2023. The rapid increase in the population, along with the construction of the nuclear power plant and various other economic initiatives, has led to rapid coastal development. However, this rapid and unplanned development has also heightened the vulnerability of the coastal areas. This research focuses on evaluating the vulnerability of this sensitive coastal zone in response to SLR. In our study, we employed the CVI method of McLaughlin and Cooper (2010), integrating seven physical and four socioeconomic parameters from various sources to conduct a comprehensive vulnerability assessment.

2 Materials and Methods

2.1 Study Area

The study area encompasses the southeastern coastal region of Türkiye, in the northeastern Mediterranean, comprising three major provinces: Mersin, Adana, and Hatay (Fig. 1). The total length of the study area's coastline is approximately 520 km. The region's high natural and socioeconomic value arises from the diverse ecosystems, population densities, residential and recreational zones, as well as from

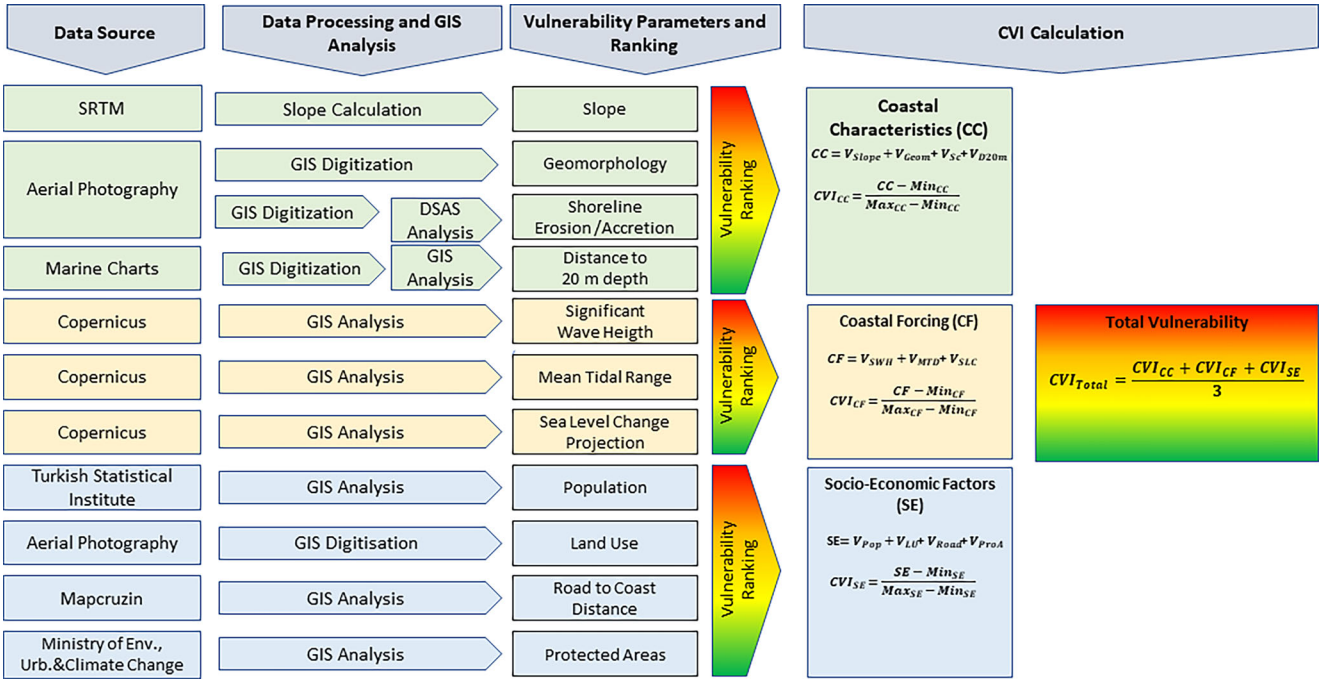

Fig. 2 Workflow of the coastal vulnerability assessment in this study. *SRTM* Shuttle Radar Topography Mission, *DSAS* Digital Shoreline Analysis System

the presence of commercial ports and industrial facilities along its coasts. The population in this region accounts for approximately 7% of Türkiye's total population and over 50% of the Mediterranean region's population (Turkish Statistical Institute 2019). In addition to densely populated coastal cities like Mersin, İskenderun, and Arsuz, the majority of the coastal zone is dotted with secondary residences, leading to a substantial rise in the population during the summer season. The region also accommodates numerous economic facilities. Besides the three major ports, the coastal zone hosts numerous industrial facilities, thermal power plants, and Türkiye's first nuclear power plant. Furthermore, the coastal plains boast fertile soils, making them ideal for cultivating high-value agricultural products like citrus, strawberries, and bananas (Turkish Statistical Institute 2018).

The region exhibits geomorphological variations from place to place. In the western part of the coastal zone, the Taurus Mountains stretch along the coastline. Alluvial plains, formed by the rivers Göksu, Seyhan, and Ceyhan, extend from Taşucu to the east along the coastal zone. In addition, these coastal plains are home to important lagoons, wetlands, and endangered species. Further east, the Amanos mountains are situated along the coast (Fig. 1).

2.2 Methodology

The methodology for assessing coastal vulnerability in this study is illustrated in Fig. 2. The evaluation process encompasses seven physical parameters: coastal slope, geomorphology, shoreline change, significant wave height, tidal range, sea level change, and distance to 20 m water depth. The first six parameters, commonly used in vulnerability assessments, offer a significant advantage due to their widespread accessibility. Palmer et al. (2011) suggest using the distance from the coast to the 20 m depth contour, as it is a critical factor in evaluating wave energy. The choice of these parameters to represent vulnerability is largely determined by the availability of data.

Additionally, four socioeconomic factors are considered: population density, land use, distance of roads to the coast, and the presence of protected areas. These parameters have been chosen because they encompass a broad range of human activities and infrastructure, as well as significant natural reserves, which collectively increase the vulnerability of coastal areas.

All these parameters are derived through a series of analyses in a GIS environment, utilizing diverse data sources (Fig. 2). Each parameter is then assigned a vulnerability rating ranging from low to high. Following this, three sub-indices are calculated based on these parameters, employing a method developed by McLaughlin and Cooper (2010). The overall coastal vulnerability index is then determined as the mean of these three sub-indices (Fig. 2).

Table 1 The vulnerability classification of physical and socioeconomic parameters

Sub-index	Parameters/ vulnerability	Low (green)	Moderate (yellow)	High (orange)	Very high (red)
		1	2	3	4
Coastal characteristic	Coastal slope (degree)	>10	10–4	4–1	<1
	Geomorphology	Cliff, rocky	Alluvial plains	Beach	Estuary, delta, lagoon
	Distance to 20 m water depth (km)	>4	2–4	1–2	<1
	Shoreline change (m)	>1	0–−1	–1–−5	<–5
Coastal forcing	Significant wave Height (m)	<1.15	1.15–1.40	1.40–1.85	>1.85
	Tidal range (m)	–	–	>0.33	<0.33
	Sea level change projection (m)	–	<0.55	0.55–0.58	>0.58
Socioeconomic factors	Population (people/0.01 km^2)	0–20	20–100	100–200	200–300
	Land use	Water bodies, unclaimed	Lagoon, forest	Agriculture, discontinuous urban, beach	Continuous urban, industrial units, ports
	Road to coast distance (km)	>2	0.5–2	0.2–0.5	<0.2
	Protected area	Absent	–	–	Present

2.2.1 Coastal Vulnerability Index

In this study the CVI method developed by McLaughlin and Cooper (2010) was used to assess the vulnerability of the coastal zone. This method assesses physical and socioeconomic parameters separately.

This CVI consists of three distinct sub-indices: (1) a coastal characteristics sub-index, evaluating the coast's erosion resilience and susceptibility; (2) a coastal forcing sub-index, outlining factors influencing wave-induced erosion; and (3) a socioeconomic sub-index, pinpointing targets such as population, land use, and infrastructure at high risk. In this methodology, parameters are assigned a ranking on a scale from 1 to 4, indicating their impact on coastal vulnerability, with 4 representing the highest and 1 the lowest impact. The ranking matrix for these sub-index variables is detailed in Table 1 for this study.

$$\text{Addition of Sub-Index} = X_1 + X_2 + X_3 + \ldots + X_n \quad (1)$$

$$\text{CVI}_{\text{Sub-Index}} = \frac{[\text{Addition of Sub-Index}] - \text{Minimum}_{\text{Addition of Sub-Index}}}{\text{Maximum}_{\text{Addition of Sub-Index}} - \text{Minimum}_{\text{Addition of Sub-Index}}} \times 100 \quad (2)$$

$$\text{CVI}_{\text{Index}} = \frac{\text{CVI}_{\text{Sub-Index}_a} + \text{CVI}_{\text{Sub-Index}_b} + \text{CVI}_{\text{Sub-Index}_c}}{3} \quad (3)$$

where X_1, X_2, ..., X_n represent the numerical values of parameters, while CVI sub-indices a, b, and c correspond to coastal forcing, coastal characteristics, and socioeconomic indices, respectively. The first step involves summing the numerical values of the parameters for each sub-index (Eq. 1). Next, the results are normalized by calculating them as a percentage of the maximum and minimum achievable scores for each sub-index (Eq. 2). Finally, to determine the total CVI value, the average of the three sub-indices is calculated (Eq. 3).

2.3 Physical Data

The coastal characteristic and coastal forcing physical data used in this study are presented separately in Figs. 3 and 4 respectively.

Coastal slope data (Fig. 3) were generated from the 1 arc-second (30 m) resolution Shuttle Radar Topography Mission (SRTM) global elevation data, which is freely accessible at https://earthexplorer.usgs.gov. The slope calculations were performed using the Slope tool in ArcGIS Pro 3.2 (Environmental Systems Research Institute, 2023) software.

Geomorphological data (Fig. 3) were digitized from high-resolution satellite images in Google Earth, categorizing as rocky, cliff, alluvial plains, beach, estuary, delta, and lagoon. Vector polygon data obtained from Google Earth were converted to raster format using ESRI ArcGIS software.

For the shoreline erosion/accretion rate (Fig. 3), coastlines from various dates were digitized using ESRI's Wayback World Imagery, a digital archive offering access to his-

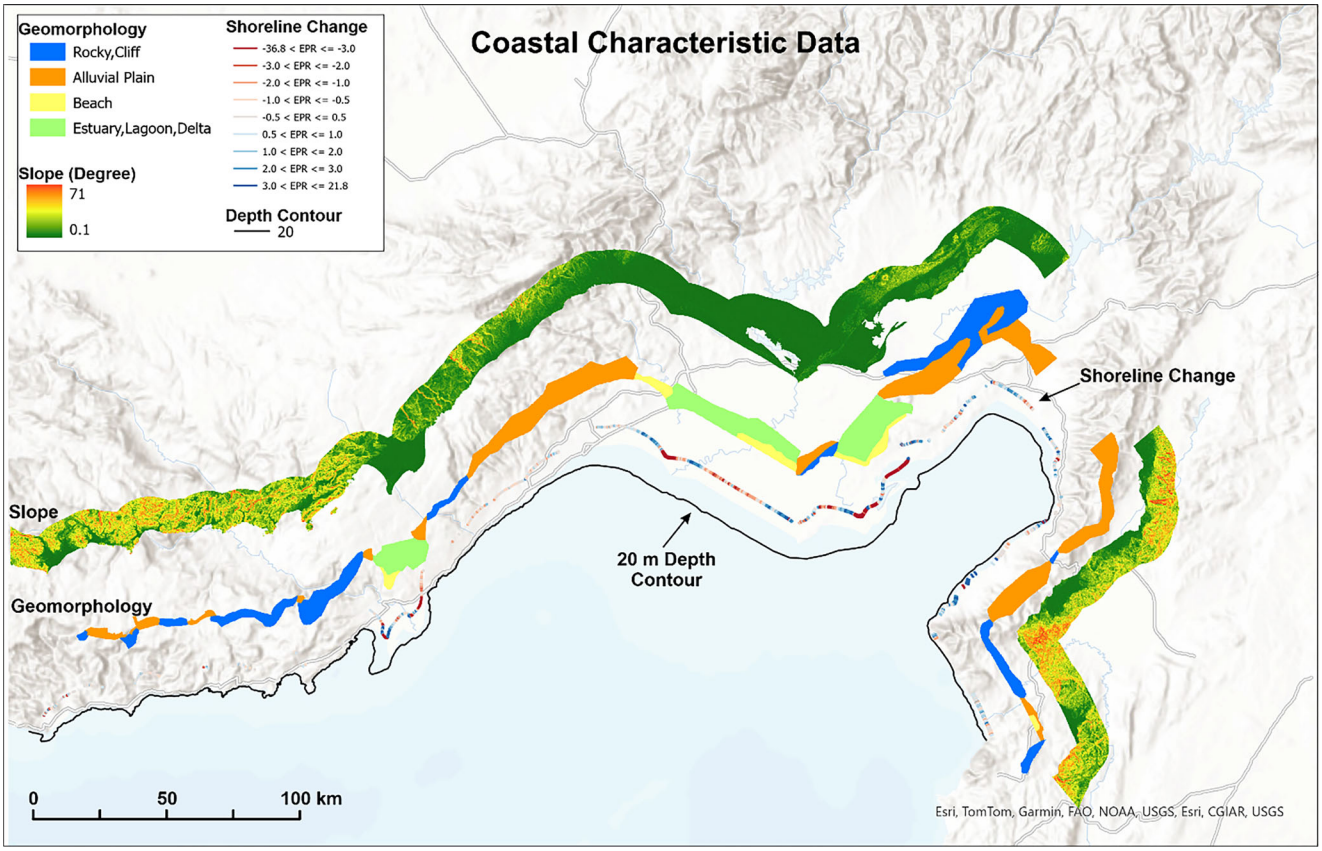

Fig. 3 Coastal characteristic (coastal slope, geomorphology, shoreline change, and 20 m depth contour) data used in this study for the coastal vulnerability assessment

torical World Imagery versions of ESRI (https://livingatlas.arcgis.com/wayback). Each version includes maps from before its publication date, allowing for comparative analysis of coastlines at different times and locations. The study utilized digitized coastlines spanning from 2006 to 2022. For each segment of the study area, at least two corresponding maps were analyzed. The study processes digitized historical coastlines using the Digital Shoreline Analysis System (DSAS) software to calculate shoreline change rates, applying the baseline method (Leatherman and Clow 1983). A baseline, established parallel to the coastline, guides the creation of perpendicular transects intersecting each historical shoreline. These transects, strategically positioned at 200-meter intervals along the coast, facilitate a systematic analysis of shoreline changes. The end point rate (EPR) model (Himmelstoss et al. 2018) is employed to calculate the shoreline change rate. This model is preferred for its computational simplicity and its minimal requirement of just two shoreline dates for analysis, as detailed by Thieler et al. (2009). For the calculation, a suggested default data uncertainty value of 10 m, as recommended by Himmelstoss et al. (2018), is utilized.

The distance to the 20 m depth contour (Fig. 3) was determined by locating the closest point of the 20 m isobath to the coastline, utilizing bathymetric data obtained from marine hydrographic charts of the region.

Significant wave height is regarded as an indicator of vulnerability, contributing to land loss through increased erosion and flooding along the coast. This parameter represents the average height of the highest third of ocean or sea surface waves, which are primarily generated by wind and swell. Significant wave height data were obtained from the "Ocean surface wave indicators for the European coast from 1977 to 2100 derived from climate projections" dataset that was produced on behalf of the Copernicus Climate Change Service (Caires and Yan 2020). The dataset employed in this study (Fig. 4) is based on the 90th percentile of significant wave height for ERA5 reanalysis, specifically focusing on the period from 2001 to 2017 (Fig. 3). The dataset is available in the Climate Data Store of Copernicus at https://cds.climate.copernicus.eu/.

Tidal range data and mean sea level data were acquired from the "Water level change indicators for the European coast from 1977 to 2100 derived from climate projections" dataset that was produced on behalf of the Copernicus Climate Change Service (Yan et al. 2020). The dataset is available in the Climate Data Store of Copernicus at https://cds.climate.copernicus.eu/.

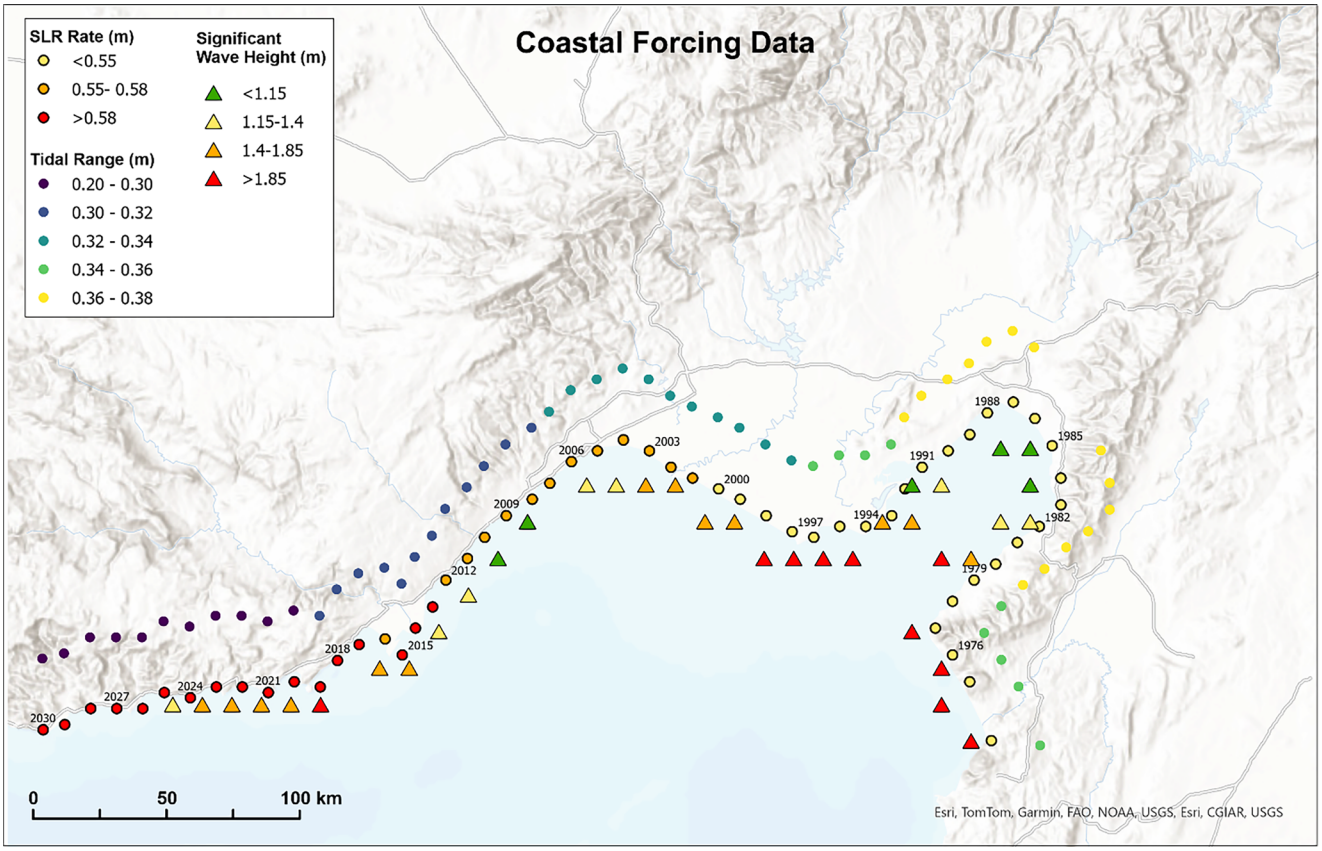

Fig. 4 Coastal forcing (significant wave height, SLR rate, and tidal range) data used in this study for the coastal vulnerability assessment. The numbers are the station IDs for SLR and tidal range datasets

For our analysis, we apply model results projected for 2041–2070 under a pessimistic climate scenario, often referred to as the business-as-usual scenario (RCP8.5), where emissions continue to increase throughout the century (Yan et al. 2020). In this study, we utilize tidal range and mean sea level data projected under the RCP8.5 climate scenario at 57 strategically positioned stations at 0.1-degree intervals along the coastline (Fig. 4).

Tidal range data for each station over a 29-year period under the RCP8.5 climate scenario is characterized by a single averaged value, from which the impact of sea level rise has been excluded. This approach isolates the tide and its variations for pure characterization (Yan et al. 2020).

The mean sea level data encompass the sea level rise observed during a simulated 30-year period. This dataset does not include the impact of storm surges caused by atmospheric forces. In this study, we calculated the annual sea level rise (SLR) rate using projected mean sea level data from 2041 to 2070 for 57 stations, as shown in Fig. 4.

2.4 Socioeconomic Data

The socioeconomic data relevant to this study are depicted in Fig. 5.

Population information was sourced from the Turkish Statistical Institute (Turkish Statistical Institute 2022). The data (Fig. 5) cover all the neighborhoods in the coastal zones based on the Address-Based Population Registration System (ABPRS).

Land-use data (Fig. 5) were acquired through analysis of satellite images using Google Earth software (Aykut 2021). Coastal areas were digitized and classified into categories such as agricultural land, beaches, urban areas (both continuous and discontinuous), forests, industrial units, lagoons, ports or piers, unclaimed areas, and water bodies. These land-use types were further categorized into four groups based on their vulnerability to SLR for the vulnerability index.

Road vector data for the study area, as shown in Fig. 5, were obtained from Mapcruzin web site (https://mapcruzin.com/free-turkey-arcgis-maps-shapefiles.htm). These data were then cross-referenced with digital maps from the General Directorate of Highways to ensure thorough cross-verification.

The protected areas, defined by the International Union for Conservation of Nature (IUCN), are specific geographic regions managed under legal guidelines to preserve biological diversity, natural resources, and related cultural heritage.

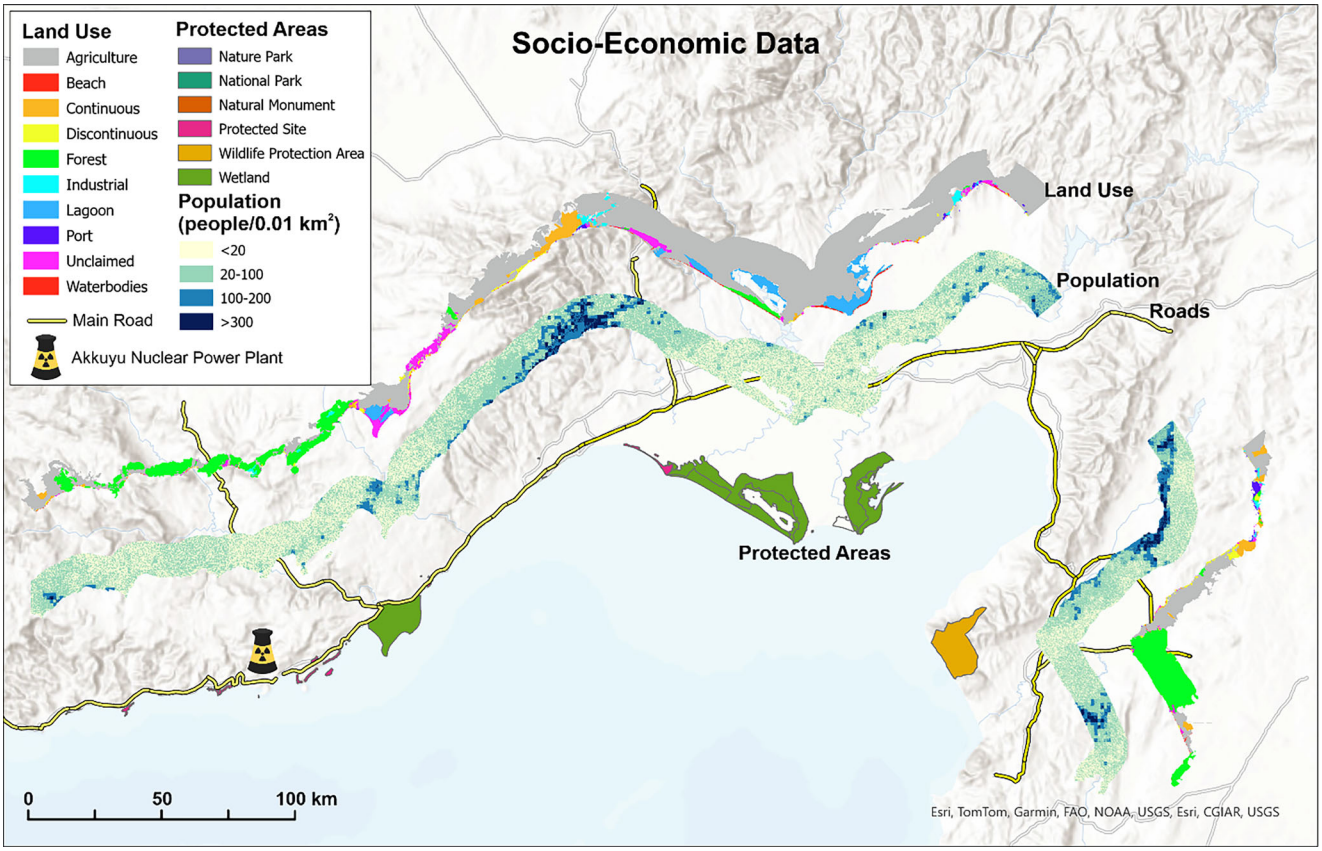

Fig. 5 Socioeconomic (population, land use, roads, and protected area) data used for coastal vulnerability assessment

In Türkiye, the responsibility for implementing protection regulations falls under the Ministry of Environment, Urbanization, and Climate Change, as well as the Ministry of Agriculture and Forestry. These protected areas are categorized as national parks, nature parks, nature monuments, nature conservation areas, wildlife conservation areas, Ramsar areas, wetlands, protection forests, city forests, gene conservation forests, seed orchards, and seed stands. The information regarding protected areas in the research region is sourced from the GIS portal of the Ministry of Environment, Urbanization, and Climate Change. These data include wildlife conservation areas, national parks, nature parks, and two Ramsar sites located along the coast of the study area (Fig. 5).

2.5 CVI Parameters Ranking and Calculation

This research evaluates coastal vulnerability by employing a combination of physical and socioeconomic parameters. The physical parameters are categorized into two sections: coastal characteristics (including coastal slope, geomorphology, shoreline change, and proximity to 20 m water depth) and coastal forces (such as significant wave height, tidal range, and relative sea level change). The socioeconomic parameters encompass population, land use, roads, and protected areas.

The impacts of climate change on coastal regions, such as SLR, extend beyond the immediate coastline, affecting inland areas as well. McLaughlin and Cooper (2010) defined the inland boundary of the coastal zone as 1 km for all spatial scales in their study. However, this approach averages values across the entire buffer zone, which could potentially alter the representation of processes occurring right at the coast. Consequently, in this study, a narrower 500-meter buffer zone from the coastline inland has been adopted for the coastal vulnerability assessment. This decision aims to provide a more precise evaluation of coastal processes and their vulnerabilities.

Data for each parameter may be either qualitative or quantitative and are often available in various scales and units of measurement. To assess their contributions to vulnerability, variables are typically assigned ranks ranging from 1 (very low vulnerability) to 4 (very high vulnerability) as shown in Table 1.

The ranking of coastal characteristic parameters, including slope, geomorphology, and shoreline change, aligns with the methodologies employed in similar studies world-

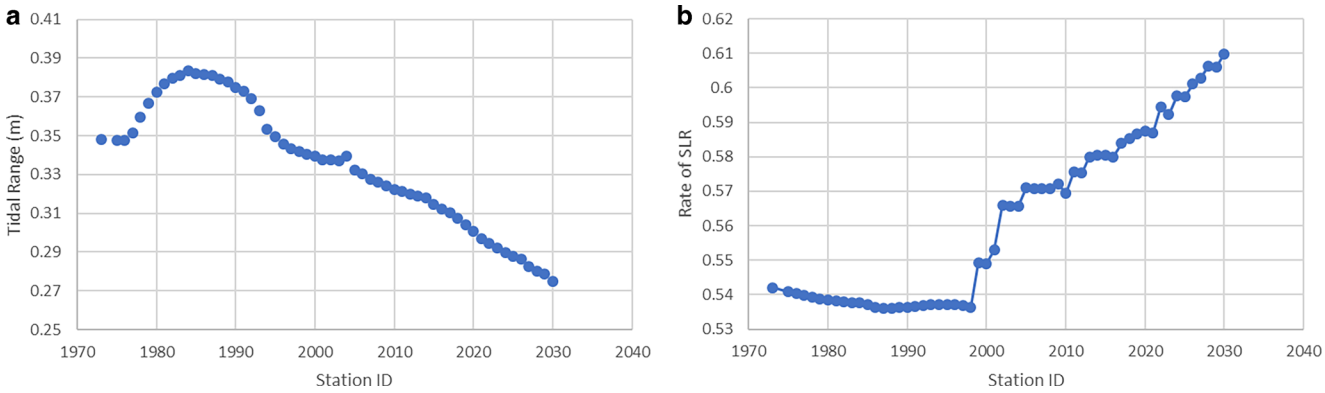

Fig. 6 **a** Average tidal range and **b** projected SLR rates according to the Copernicus model for 2041–2070 (Yan et al. 2020). Station IDs, plotted along the horizontal axis, indicate the specific locations for model calculations. Refer to Fig. 4 for a detailed map of these station locations

wide. The ranking of the distance to 20 m water depth follows the methodology established by Palmer et al. (2011).

In the vulnerability assessment for tidal range, model outcomes are displayed through a scatter graph (Fig. 6a), which aligns average range data from various stations in an east-to-west sequence. This graph demonstrates a notable divergence in data points around station 2005, marking a significant shift in tidal range measurements. Consequently, this distinct variation serves as a basis for classification, emphasizing its critical role in analyzing and understanding the region's vulnerability to tidal changes. The rate of SLR is derived from the projections of the model results (Yan et al. 2020). Figure 6b displays the SLR rate for each station. Based on the data shown in this figure, vulnerability classes for SLR have been determined. The ranking of socioeconomic parameters primarily reflects the adaptation of methodologies from previous studies to the regional context.

For vulnerability calculations, all data types were converted into a raster format with 100-meter resolution within the 500-meter buffer zone using ESRI ArcGIS software. The ranking and CVI calculations were performed using model builder in ESRI ArcGIS software.

Final CVI values were classified according to the values of 100 × 100 m grid cells within the 500-meter buffer zone from 1 to 4, from low vulnerability to high vulnerability. In this classification, CVI result values were divided into four vulnerability classes using the natural break method. The natural breaks algorithm, as described by Chen et al. (2013), is designed to minimize deviation within classes while maximizing the standard deviation between classes. This algorithm has been widely utilized in various vulnerability assessment studies (Karymbalis et al. 2012; Chen et al. 2013; Tanim and Goharian 2023, Tanim et al. 2022; Yahia Meddah et al. 2023; Dada et al. 2024).

3 Results

3.1 Coastal Characteristic Parameters

The coastal characteristics parameters, including the vulnerability ranking as a percentage of the total coastline and the corresponding coast length, are presented in Fig. 7.

3.1.1 Coastal Slope

The coastal slope parameter is used to evaluate the risk of inundation and flooding, as well as to estimate the potential rate of coastline retreat (Nageswara Rao et al. 2008). Steeper areas experience slower retreat, while low-sloping areas retreat more rapidly.

According to the slope parameter, the delta plains situated at the mouths of rivers such as Göksu, Berdan, and Ceyhan are identified as the majority of the very high-risk zones (Fig. 7). These areas are highly vulnerable due to their flat topography. Areas of high vulnerability typically include low-lying coastal plains with slopes ranging from 1 to 4 degrees. Conversely, areas with low vulnerability, characterized by steeper slopes such as coastal cliffs or rocky coasts, are mainly located in the western (e.g., Aydıncık, Yeşilovacık) and eastern (e.g., Samandag, Yayladağı) parts of the study area (Fig. 7).

3.1.2 Geomorphology

Coastal areas exhibit varying degrees of resistance to natural impacts based on their landforms. Areas prone to erosion, such as estuaries and deltas, are at greatest risk, whereas more resilient landforms like rocks and cliffs exhibit lower susceptibility to erosion.

The study identifies areas of varying vulnerability along the coast based on their landforms (Fig. 7). Coastal areas with rocky cliffs, especially between Aydıncık and Erdemli in the west and around Yayladağı in the east, exhibit low

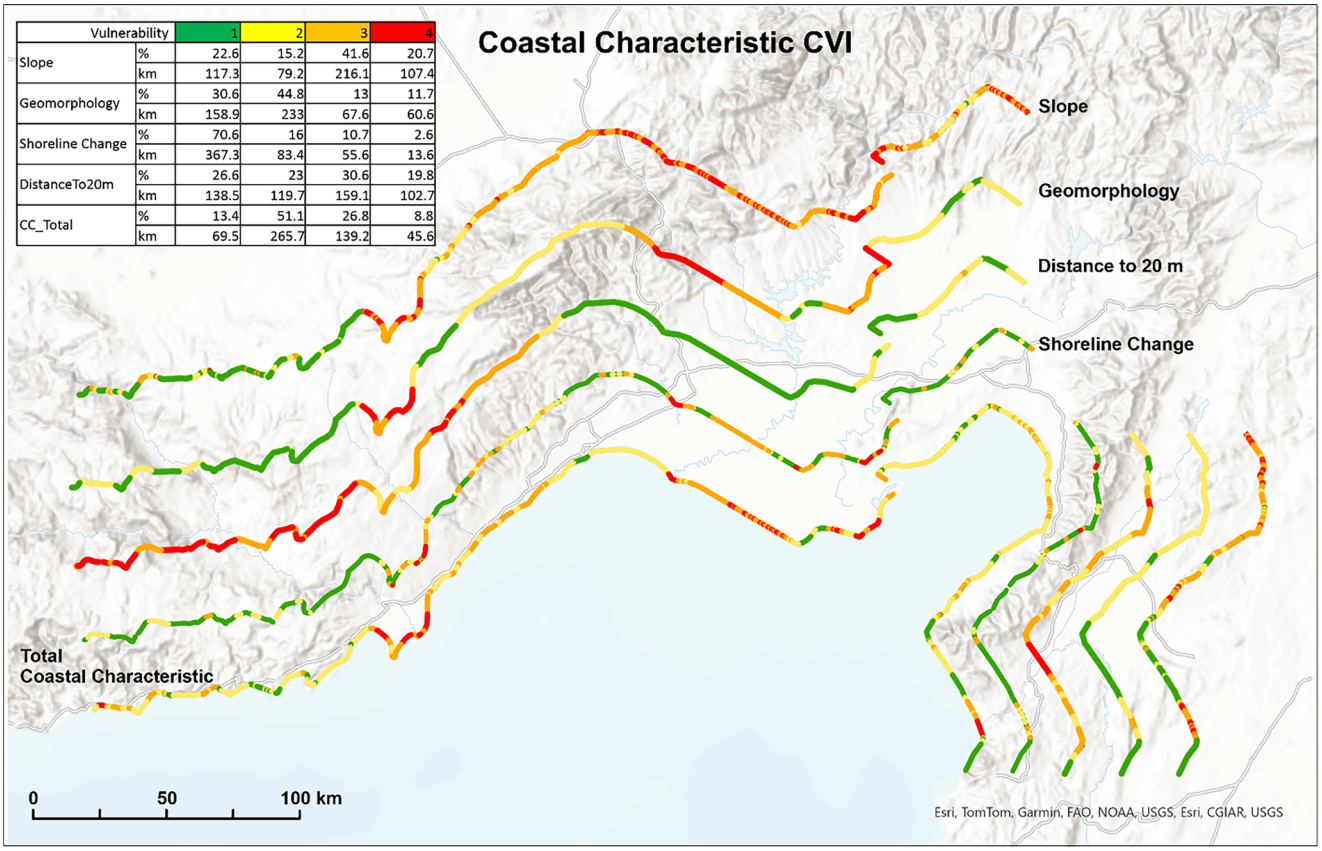

Vulnerability		1	2	3	4
Slope	%	22.6	15.2	41.6	20.7
	km	117.3	79.2	216.1	107.4
Geomorphology	%	30.6	44.8	13	11.7
	km	158.9	233	67.6	60.6
Shoreline Change	%	70.6	16	10.7	2.6
	km	367.3	83.4	55.6	13.6
DistanceTo20m	%	26.6	23	30.6	19.8
	km	138.5	119.7	159.1	102.7
CC_Total	%	13.4	51.1	26.8	8.8
	km	69.5	265.7	139.2	45.6

Fig. 7 Vulnerability classification map of coastal characteristics parameters and ranking distribution along the coast

vulnerability. Alluvial plains, which are prevalent in the region, including the Mersin and Yumurtalık plains, are classified as moderately vulnerable. Beaches, due to their sensitive nature, are considered highly vulnerable. The most vulnerable areas, categorized as very highly vulnerable, include coastal regions with landforms prone to erosion, such as estuaries, lagoons, and deltas. These are particularly noted in the wetland zones of Yumurtalık, Tarsus, and Silifke (Fig. 7).

3.1.3 Distance to 20 m Water Depth

In coastal vulnerability assessments, the distance to the 20 m water depth is a key factor in evaluating wave energy. As the distance increases, wave energy dissipates more, leading to a reduction in the erosive power of the waves (Mather et al. 2010) and consequently lowering the shoreline's vulnerability to the effects of extreme weather conditions (Davies 2012).

This study applies the vulnerability ranking developed by Palmer et al. (2011) to assess the vulnerability of different coastal areas, as outlined in Table 1. The eastern and western parts of the study area are identified as having high to very high vulnerability, consistent with their geomorphological characteristics. Conversely, the northern part, characterized by a very gentle seafloor slope, is classified as having low vulnerability (Fig. 7).

3.1.4 Shoreline Change

Historical coastlines from various dates, obtained from ESRI's Wayback World Imagery, have been processed using DSAS (Digital Shoreline Analysis System) software. This process is used to determine the rate of shoreline change, including both erosion and accretion, along the coast.

In the study region, certain coastal areas have been identified as depositional zones, formed by sediment accumulation from the Göksu, Seyhan, and Ceyhan rivers. These areas are classified as having low vulnerability (Fig. 7). Conversely, coastal regions experiencing significant erosion are categorized as very highly vulnerable, with the main erosional zones located in the Göksu Delta, near the mouth of the Seyhan River, and along the northern coast, including the Akyatan Lagoon. In other parts of the region, sediment movement remains stable, showing neither permanent deposition nor significant erosion.

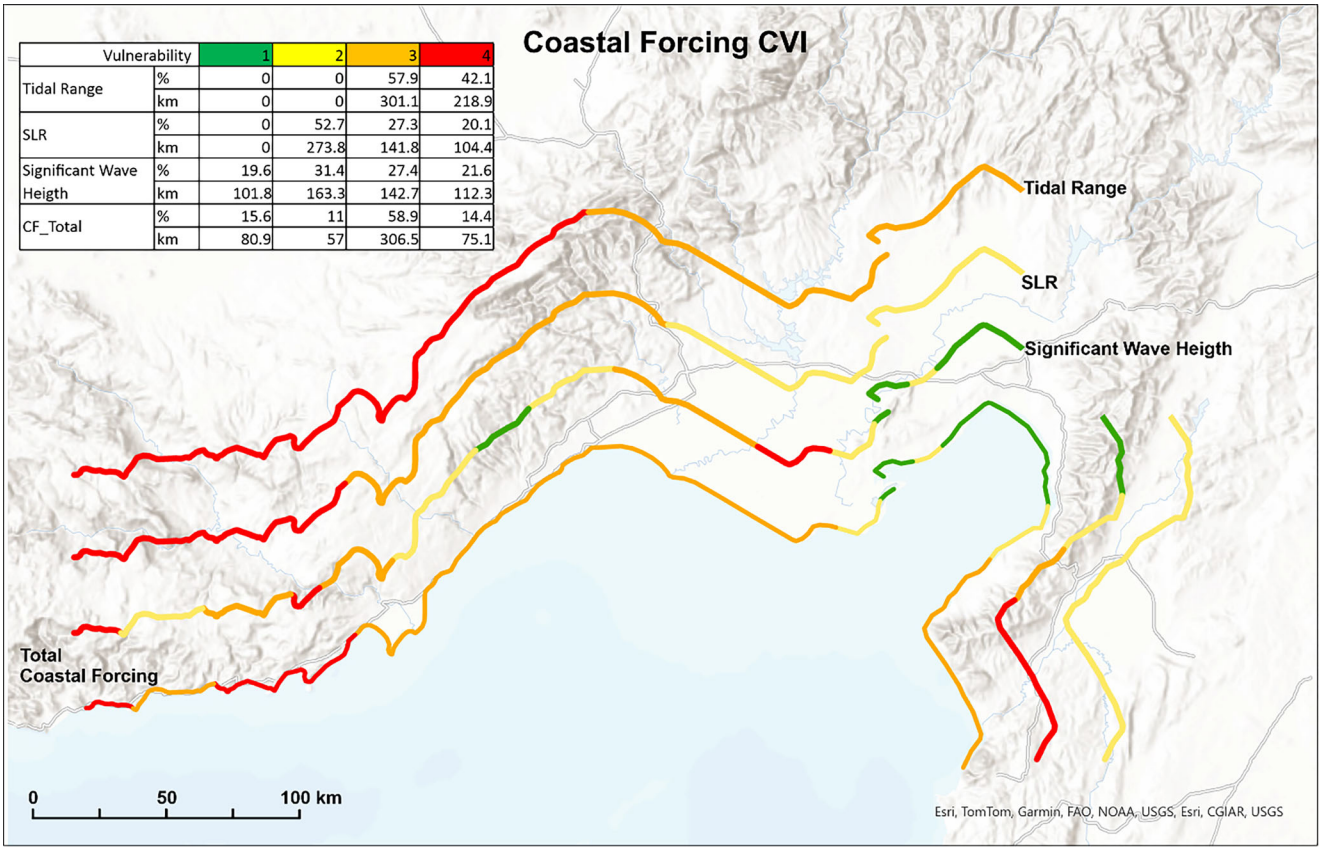

Fig. 8 Vulnerability classification map of coastal forcing parameters and ranking distribution along the coast

3.2 Coastal Forcing Parameters

Figure 8 displays the coastal forcing parameters, detailing the vulnerability ranking as a percentage of the total coastline along with the respective lengths of the coast.

3.2.1 Significant Wave Height

Waves play a crucial role in driving sediment transport along coastlines, resulting in both erosion and deposition. Based on significant wave height, areas of low vulnerability are primarily located in the inner part of İskenderun Bay (Fig. 8). The moderately vulnerable areas consist of coastal plains mainly found between Silifke and Mersin. Areas of high vulnerability are primarily situated along the northern coast, while areas of very high vulnerability are predominantly located in the southeastern part of the region (Fig. 8).

3.2.2 Mean Tidal Range

The study region is categorized as a micro-tidal coastal region, attributed to the minimal difference between its high and low tides. The consistently high sea level, coupled with the narrow tidal range, heightens the risk of erosion and inundation during storm surges. As a result, regions along the coast with low tidal ranges are deemed to be more vulnerable.

Based on the results from Copernicus' model (Yan et al. 2020), the study area is categorized into two vulnerability classes: the eastern region, including İskenderun Bay, is identified as highly vulnerable (Fig. 8); meanwhile, the coastal stretch from Anamur to Mersin is classified as very highly vulnerable (Fig. 8).

3.2.3 Mean Sea Level Change

Sea level rise, one of the primary consequences of climate change, poses a significant threat to coastal areas. Satellite altimetry data clearly illustrate the substantial increase in sea levels in the Eastern Mediterranean. The relative sea level rise encompasses various local effects in coastal regions, including atmospheric pressure, steric effects, and local land movements.

Despite reports of tectonic subsidence in the study region, with rates between 0.26 and 0.3 m per 1000 years (Aksu et al. 1992), its impact is considered negligible compared to the sea level rise. Therefore, the vulnerability as-

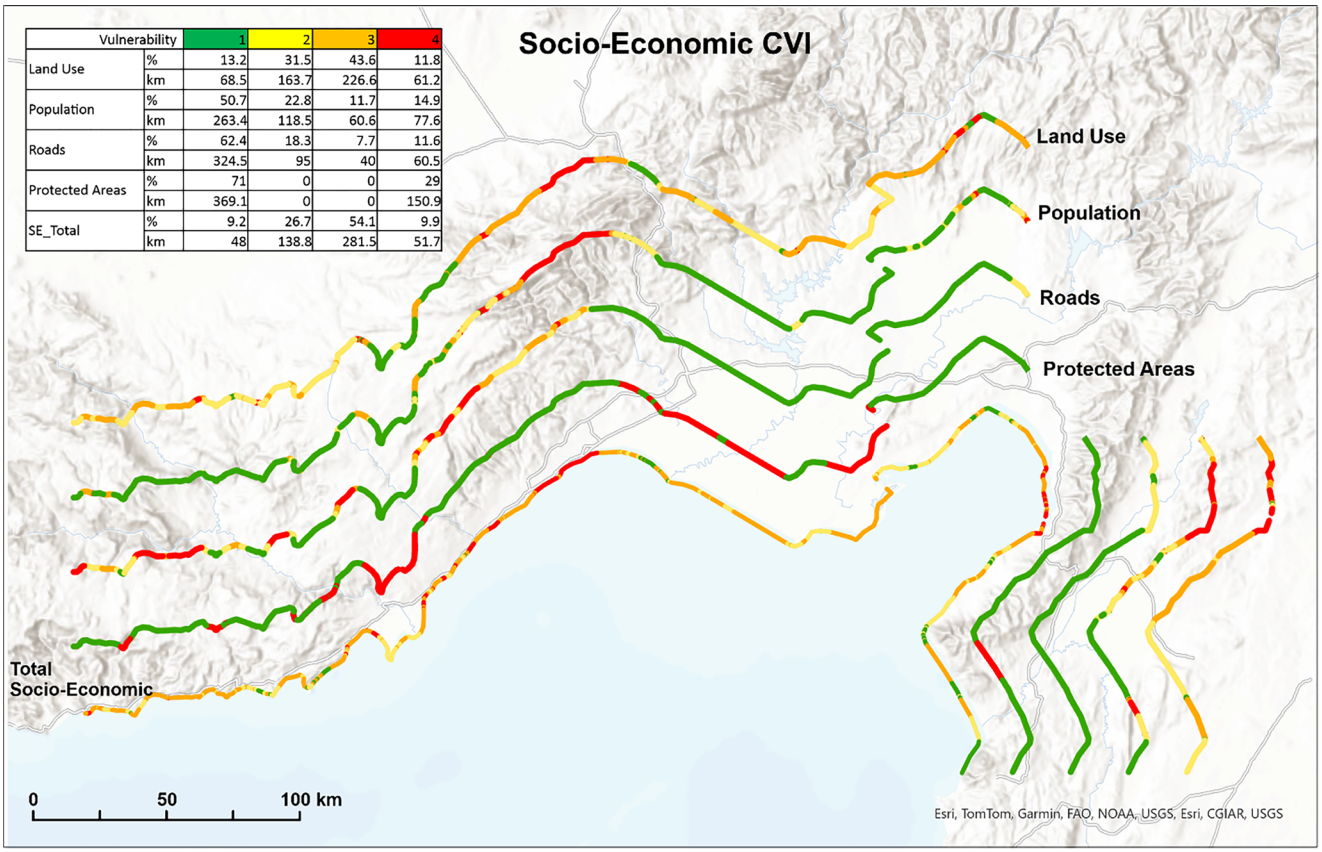

Vulnerability		1	2	3	4
Land Use	%	13.2	31.5	43.6	11.8
	km	68.5	163.7	226.6	61.2
Population	%	50.7	22.8	11.7	14.9
	km	263.4	118.5	60.6	77.6
Roads	%	62.4	18.3	7.7	11.6
	km	324.5	95	40	60.5
Protected Areas	%	71	0	0	29
	km	369.1	0	0	150.9
SE_Total	%	9.2	26.7	54.1	9.9
	km	48	138.8	281.5	51.7

Fig. 9 Vulnerability classification map of socioeconomic parameters and ranking distribution along the coast

sessment to sea level rise for this study is based on projections for 2041–2070 (Yan et al. 2020).

Based on these projections, sea level rise in the study region increases from east to west. The most significant increase is observed between Anamur and Taşucu, which is classified as very highly vulnerable. The area from Taşucu to Mersin city is considered highly vulnerable. The rest of the coast is categorized as moderately vulnerable, as shown in Fig. 8.

3.3 Socioeconomic Parameters

Figure 9 outlines the socioeconomic parameters, showing the vulnerability ranking as a percentage of the total coastline, along with the lengths of the coast corresponding to each ranking.

3.3.1 Population

The population parameter is divided into four classes based on human settlement density per 0.01 km^2. Areas with high population densities are considered the most vulnerable. The coastlines of İskenderun and Mersin cities are classified as very highly vulnerable due to their dense populations (Fig. 9). Coastal areas with sporadic, intermittent settlements are deemed highly vulnerable. Areas with scattered distribution of settlements fall into the moderately vulnerable category. The largest segment is assessed as low vulnerability.

3.3.2 Land Use

In the study region, land-use parameters are categorized into four levels of socioeconomic significance, each reflecting a distinct level of vulnerability. Areas classified as very highly vulnerable include “continuous urban,” “industrial units,” and “ports.” These are primarily located around the coasts of Mersin, Erdemli, and İskenderun, noted for their extensive urban development. Moreover, the coast between İskenderun and Yumurtalık, hosting significant industrial facilities, also falls into this category (Fig. 9).

Highly vulnerable areas, such as “agricultural land,” “discontinuous urban areas,” and “beaches” feature a mix of discontinuous urban zones and popular beaches, especially during the summer. These are found along the coasts of Erdemli, Karataş, Yumurtalık, Dörtyol, Arsuz, and Samandağ. The stretch from Mersin to Karataş is known for its industrial zones, whereas fertile lands in

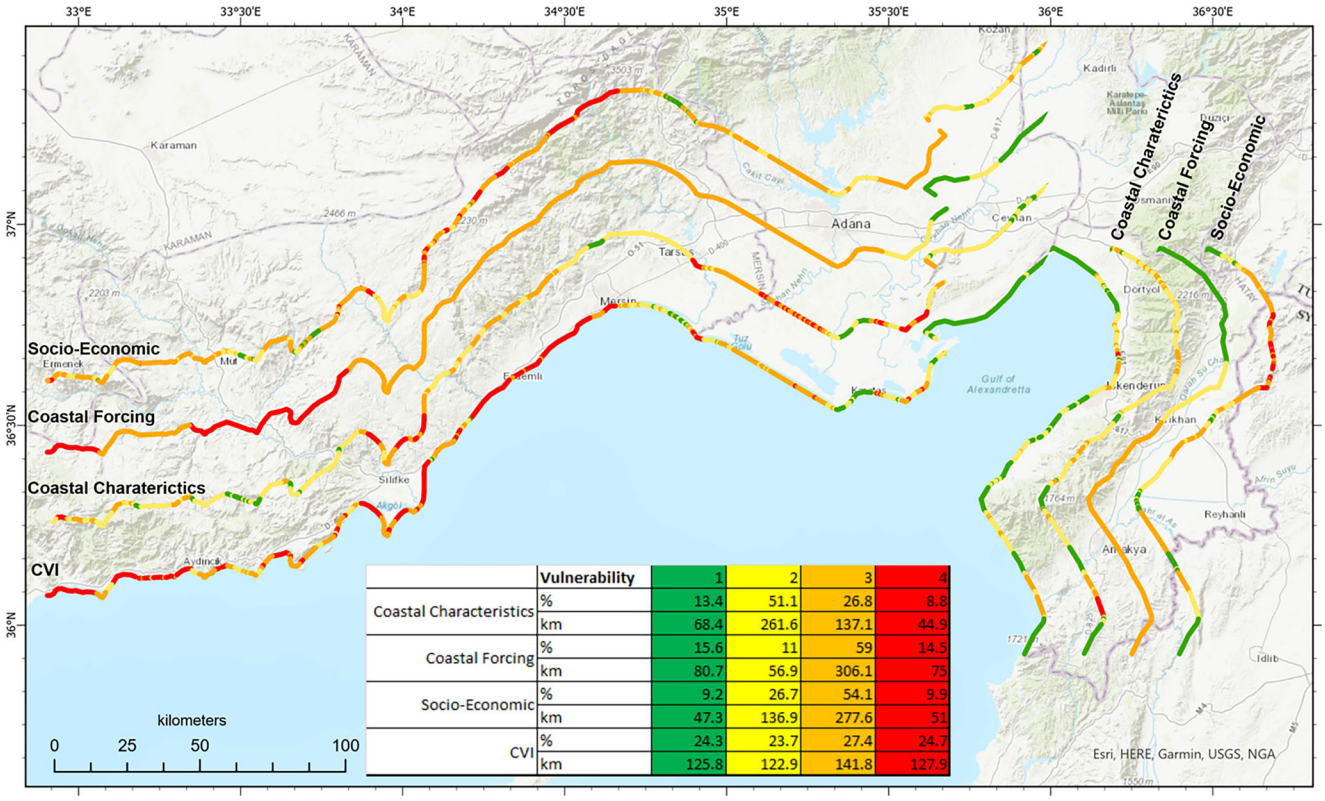

	Vulnerability	1	2	3	4
Coastal Characteristics	%	13.4	51.1	26.8	8.8
	km	68.4	261.6	137.1	44.9
Coastal Forcing	%	15.6	11	59	14.5
	km	80.7	56.9	306.1	75
Socio-Economic	%	9.2	26.7	54.1	9.9
	km	47.3	136.9	277.6	51
CVI	%	24.3	23.7	27.4	24.7
	km	125.8	122.9	141.8	127.9

Fig. 10 The coastal vulnerability index (CVI) map based on CVI sub-index method

this stretch, parts of Yumurtalık, and the area between İskenderun and Arsuz are dedicated to agriculture (Fig. 9).

"Lagoons" and "forests" fall under the moderately vulnerable category, with forests being prominent in the southwestern and southeastern parts of the region (Fig. 9).

Lastly, areas not designated for specific use are classified as "unclaimed areas," and together with "water bodies," are considered low vulnerability. A prime example of low vulnerability within the study area are the coasts of the Göksu Delta (Fig. 9).

3.3.3 Roads

Roads in close proximity to the coastline are considered more vulnerable. To classify their vulnerability, the distance between the main roads and the shoreline was measured. Based on this parameter, highly vulnerable areas are primarily found along the southwestern coast of the study region (Fig. 9).

3.3.4 Protected Areas

In the study area, a range of protected areas exist. For the purposes of this study, the presence of these protected areas categorizes the coastal zone as very high vulnerability (Fig. 9).

3.4 Coastal Vulnerability Index in the Mersin and İskenderun Bays

In this study, the coastal vulnerability index (CVI) is derived as the mean of three sub-indices: coastal characteristics, which is the nature of the coast; coastal forcing, which is the degree to which the coast is exposed to wave energy; and socioeconomic factors, which identify potential at-risk targets, as outlined by McLaughlin and Cooper (2010). Each sub-index is calculated using distinct parameters, as detailed in Table 1.

The cumulative impact of coastal characteristics results in 52.1% of the study area's coastline being classified as high to very highly vulnerable (Fig. 10). Areas of moderate vulnerability constitute 23.7% of the coastline, while regions with low vulnerability account for 13.4%.

4 Discussion

4.1 Assessment of Physical Parameter Vulnerability

Coastal characteristic parameters, including coastal slope, geomorphology, shoreline change, and distance to 20 m depth contour reveal how coastal areas, particularly in

the context of SLR, respond to climate change impacts (McLaughlin and Cooper 2010).

Coastal slope is a critical parameter when assessing the vulnerability of coastlines to natural processes like coastal erosion, inundation, and sea level rise. This is due to the fact that in the event of a SLR, areas with a gentle slope are at greater risk of extensive flooding, while steeper coastal areas are less susceptible to the impacts of rising sea levels. It is indicated that the area up to 1 m above the shoreline is at risk of permanent flooding, while the area up to 5 m high has the risk of rising above the tides in extreme storm events (Koroglu et al. 2019). In this study, the presence of extensive alluvial plains in the Adana and eastern Mersin regions significantly amplifies the area's overall vulnerability, largely due to its coastal topography (Fig. 1).

The southwestern part of the study region, influenced by the Taurus Mountains, features steep slopes in coastal areas. These steep slopes are intersected by numerous river plains, which reduce the overall steepness. Similarly, in the southeastern part, sloping areas are present where the Amanos Mountains extend into the sea (Fig. 7).

Geomorphology is linked to material resistance against sea level rise effects in coastal areas, contributing to increased vulnerability in most of the study area. The shoreline change parameter, which identifies erosional or accretional areas along the study area's coastline, has a relatively low impact on its overall vulnerability (Fig. 7).

In this study, coastal forcing, which measures the coast's exposure to wave energy (McLaughlin and Cooper 2010), comprises three parameters: significant wave height, mean tidal range, and mean sea level change.

Waves are the main driver of the sediment transport along coasts, for both erosion and deposition processes. Waves with higher wave heights carry greater energy as they approach the shore. When high-energy waves break near the shoreline, they lead to the transport of larger sediment volumes (Koroglu et al. 2019). Waves with maximum heights of 2.5 m primarily impact the Adana and southern Hatay regions in the study area.

The tidal range is the vertical difference between the highest and lowest sea levels. While some studies (Gornitz et al. 1994; Diez et al. 2007; Yin et al. 2012; Duriyapong and Nakhapakorn 2011; Addo 2013) suggest that a high tidal range is highly vulnerable to sediment transport capacity, others argue that a low tidal range increases vulnerability due to the proximity of sea levels to high tide, leading to erosion caused by waves and storm surges (Gaki-Papanastassiou et al. 2010; Karymbalis et al. 2012; Gorokhovich et al. 2014; Ozyurt and Ergin 2010).

The study area is classified as a micro-tidal coastal region due to the short range between high and low tides. This, coupled with the presence of extensive, flat coastal areas characterized by low slopes, makes the tidal range one of the key factors contributing to the area's overall vulnerability.

Relative sea level change, an essential parameter in vulnerability assessments, encompasses both global sea level changes and local influences like atmospheric pressure, steric effects, and local land movements. Although differential tectonic subsidence is documented in the Cilician Basin and İskenderun Bay (Aksu et al. 1992), the impact of such land movements is minimal enough to be disregarded. Consequently, in these vulnerability assessments, the mean sea level is the preferred metric.

Long-term evaluations of satellite altimetry data, as presented in studies by Cazenave et al. (2001) and Hebib and Mahdi (2019), consistently demonstrate a continuous rise in sea levels in the Eastern Mediterranean. Hebib and Mahdi (2019) specifically highlight an upward trend in sea levels in the coastal Mediterranean Sea throughout the altimetry period (1993–2015), noting a notable rise particularly in the Eastern Mediterranean basin.

The accuracy and reliability of climate models make them favorable for use in vulnerability assessments. In this study, we use model projections for 2041–2070 under a pessimistic climate scenario (RCP8.5), not only due to their dependability but also because of the spatial distribution of the data.

Although classified as a coastal characteristic, the distance to the 20 m depth contour is closely linked to the significant wave height parameter in coastal forcing. A larger distance typically diminishes the impact of waves on the coast. Waves primarily dissipate energy in shallow waters as a result of friction against the seabed, which simultaneously reduces their speed. Conversely, in deep waters, often exceeding half the wave's wavelength, there is no seabed interaction, enabling waves to approach the coast while retaining their full energy. For instance, in the study region's northern part, where the seabed gently deepens, the significant wave height is considered highly vulnerable, whereas the distance to the 20 m depth contour is deemed to be of low vulnerability. This contrast between the two parameters helps balance their combined effects on the overall vulnerability assessment.

4.2 Assessment of Socioeconomic Parameter Vulnerability

Population plays a pivotal role in the context of coastal vulnerability. While high population can be seen as a direct factor contributing to coastal erosion (Kunte et al. 2014; McLaughlin et al. 2002), it can also be associated with greater economic value (Hughes and Brundrit 1992) and increased investment in property protection (Hegde and Reju 2007). As a result, regions with high population densities are often regarded as more vulnerable than others. In the

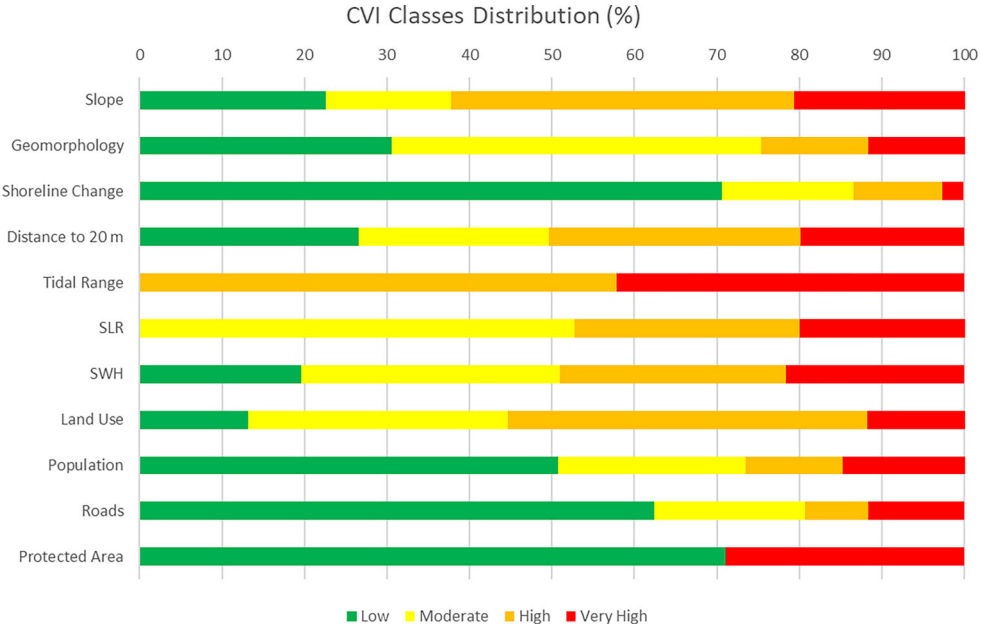

Fig. 11 The percentage distribution of different vulnerability classes—low, moderate, high, very high—across all the parameters used in this study

study area, particularly in the eastern Mersin region, high population density areas are considered more vulnerable due to a lack of sufficient coastal defense infrastructure.

Roads play a significant role in Türkiye's transportation system, driving both human and economic activities. Due to their economic significance, roads are a crucial socioeconomic parameter in assessing coastal vulnerability. In the study area, unlike the physical parameters, the presence of roads close to the shoreline makes the coasts of Hatay and western Mersin regions more vulnerable.

Protected areas serve as safe habitats for numerous plant and animal species within coastal ecosystems. Given their crucial role, these protected coastal areas are assessed as highly vulnerable to the impacts of climate change. In the study area, one third of the coastline consists of protected areas, making it particularly vulnerable.

4.3 The Coastal Vulnerability Assessment

Numerous CVI studies have been conducted worldwide, employing various parameters. However, the extent of variability in these parameters within a study region can vary significantly. This variation can be attributed to whether the data for these parameters are expressed quantitatively or qualitatively. Notably, parameters categorized numerically tend to exhibit more variability, while some parameters remain constant throughout the entire region, maintaining the same value and class.

In this study, a total of 11 parameters were utilized. Among these parameters, coastal slope, geomorphology, land use, population, coastal erosion, and distance to 20 m depth contour exhibited higher variability within the study region, exerting a significant influence on the CVI results (Fig. 11). Protected areas, roads, and significant wave height, while containing some regional variations, also contributed to the CVI values. Notably, protected areas and roads parameters can wield a substantial impact on CVI results due to their socioeconomic significance in some CVI calculation methods. However, although mean sea level and tidal range parameters have variations in studies conducted in various locations around the world, they are less variable compared to other parameters in the study region (Fig. 11). Therefore, their relationships with CVI result values are weaker than those of other parameters.

The Mersin region, spanning from Anamur to Mersin city, constitutes the western part of the study area. The western sections of the Mersin region's coastline are predominantly categorized as having low to high vulnerability across all parameters. Conversely, the eastern portions exhibit greater vulnerability compared to their western counterparts. This heightened vulnerability is attributed to factors such as lower slopes, weaker geological formations, land-use patterns, and higher population density in the eastern regions. Additionally, the proximity of the Taurus Mountains to the coastline and steeper coastal terrain in western Mersin discourage extensive human utilization of these coastal areas.

The Mersin region coast has the highest population density in the entire study area. Additionally, the presence of the crucial Mersin port, facilitating international sea transportation, makes this region vulnerable in terms of land use. Along the shores of the Mersin region, numerous tourist facilities, primarily active during the summer, contribute to a seasonal population surge. These factors collectively classify these coastal areas as very highly or highly vulnerable.

The Göksu Delta, formed by the Göksu River, is a significant feature in the Mersin region. Its low slope, deltaic geological formation, and the protected area status increase its vulnerability. On the other hand, the areas surrounding the mouth of the Göksu River, as well as some adjacent areas, are depositional areas due to the deposition of sediment transported by the Göksu River. The lack of erosion decreases the vulnerability. Furthermore, as noted by Ozyurt and Ergin (2010), specific protected areas like the Göksu Delta, subject to strict controls regarding land use and settlement, reduce the risk of vulnerability.

The Adana region, which stretches from Mersin City to Dörtyol, encompasses the flattest coastal areas in the study area. Based on the physical parameters, the whole region is classified as highly to very highly vulnerable. Despite the low population and lack of roads, the presence of extensive agricultural zones and industrial sites raise the vulnerability of the region. The presence of alluvial deltas, wetlands, and natural protected areas contributes to the increased vulnerability of the Adana region.

The Hatay region, spanning from Dörtyol to Yayladağı, is primarily characterized as having low to moderate vulnerability. Despite the significance of land-use and population parameters along these coasts, other socioeconomic and physical factors contribute to the region's overall resilience. The absence of roads and protected areas in the region lowers the vulnerability score within the socioeconomic sub-index. Notably, a wildlife conservation area between Samandağ and Arsuz is rated as very highly vulnerable in terms of the protected area parameter. Nevertheless, this single parameter does not significantly impact the CVI sub-index result score.

Several studies have yielded results that align with our research findings. Kurt and Li (2020) have reported that while the rise in sea levels along the Turkish coast may not be as significant as in other parts of the world, local vulnerabilities such as topographical features and subsidence present substantial risks. Their analysis specifically identifies the coastal areas of Adana as being at a heightened risk of inundation due to SLR. Similarly, Simav et al.'s 2013 study on the Çukurova Delta projects that by 2100, around 69% of the area will be at risk of flooding, with nearshore settlements, lagoons, and agricultural lands facing the most severe impacts of inundation.

Kuleli's (2010) study highlights that the areas most susceptible to significant land losses due to sea level rise are located along the east Mediterranean coast, specifically including Samandağ, the Çukurova Delta Plain, and the Göksu Delta.

Conversely, Kahraman and Sılaydın Aydın and Kahraman (2016) found that Mersin city exhibits a lower vulnerability to such changes. It is crucial to highlight that their research focused mainly on city centers and noted the presence of coastal protection structures along Mersin's shoreline, potentially mitigating the city's risk.

In the same study region, Aykut (2021) conducted a preliminary assessment of coastal vulnerability. Aykut (2021) provided a more quantitative ranking of parameters such as shoreline change and road presence, categorizing them simply as absent or present. This study, however, reveals a broader variation in the impact of these parameters, indicating a more complex influence on coastal vulnerability than previously understood.

5 Conclusion

Coastal regions around the world are critical for human settlements, economic endeavors, and the preservation of coastal ecosystems. These areas are increasingly under threat from climate change-induced phenomena, especially SLR. The southeastern coast of Türkiye is an example of such vulnerable landscapes, with its expansive low-lying areas, river deltas, and ecologically significant natural preserves, all of which are susceptible to the escalating threats posed by global climate change, most notably SLR.

The coastal area under study is economically important, hosting tourist attractions, farms, industrial zones, and thermal power plants, including Türkiye's first nuclear power facility which is currently being built. Simultaneously, the region's population has surged, fueled by immigrants, refugees from conflict zones, and earthquake displacements. This fast population growth, coupled with the nuclear plant construction and other economic developments, has spurred swift coastal expansion, increasing the area's vulnerability.

Considering these factors, the insights from this research provide essential guidance for local authorities and policymakers to develop informed and strategic plans for the sustainable management of coastal areas.

This research evaluated the susceptibility of Mersin and İskenderun Bay coastlines to the SLR by employing the coastal vulnerability index. This index incorporates an array of factors, including coastal dynamics, physical geography, and socioeconomic elements.

The results indicate that significant portions of the coastlines along the study region, spanning 141.8 km with high vulnerability and 127.9 km with very high vulnerability, are especially susceptible to natural disturbances. This susceptibility is primarily due to gentle slopes, fragile geomorphic structures, and erosion-prone coastal plains and deltas. These factors render the areas highly sensitive to SLR, erosion, and potential flooding. Moreover, these areas of vulnerability also coincide with zones of significant socioeconomic importance, including protected regions and hubs of

social and economic activity, intensifying their risk exposure.

Acknowledgements This manuscript is based on an updated version of the first author's Master of Science (MSc) thesis. The original thesis has been significantly revised and expanded to include new data, methodologies, and analyses, reflecting the latest research findings and advancements in the field. The authors express their gratitude to the editor and reviewers for their valuable feedback and suggestions, which greatly contributed to enhancing the quality of the paper.

Funding The authors acknowledge support from DEKOSIM (BAP-08-11-DPT2012K120880) funded by the Turkish Ministry of Development.

Author Contribution F. Aykut: Conceptualization, data interpretation, writing and editing, visualization, and discussion; D. Tezcan: Conceptualization, data interpretation, writing and editing, visualization, and discussion.

Funding Open access funding provided by the Scientific and Technological Research Council of Türkiye (TÜBİTAK).

Conflict of interest F. Aykut and D. Tezcan declare that they have no conflict of interests.

References

Addo K (2013) Assessing coastal vulnerability index to climate change: the case of Accra—Ghana, Proceedings 12th International Coastal Symposium (Plymouth, England). J Coast Res 65(Suppl):1892–1897

Aksu AE, Calon TJ, Piper DJW, Turgut S, Izdar EK (1992) Architecture of late orogenic basins in the eastern mediterranean sea. Tectonophysics 210:191–213

Aykut F (2021) Coastal Vulnerabılıty Assessment For Mersin And İskenderun Bays, Northeastern Mediterranean. MSc Thesis, Middle East Technical University. https://open.metu.edu.tr/bitstream/handle/11511/89506/FahriAykutMsThesis_final.pdf

Boruff BJ, Emrich C, Cutter SL (2005) Erosion hazard vulnerability of US coastal counties. J Coast Res 21:932–942

Caires S, Yan K (2020) Ocean surface wave indicators for the European coast from 1977 to 2100 derived from climate projections. Copernicus Climate Change Service (C3S) Climate Data Store (CDS) https://doi.org/10.24381/cds.1a072dd6

Cazenave A, Cabanes C, Dominh K, Mangiarotti S (2001) Recent sea level change in the Mediterranean Sea revealed by Topex/Poseidon satellite altimetry. Geophys Res Lett 28(8):1607–1710

Charuka B, Angnuureng DB, Brempong EK, Agblorti SK, Agyakwa AKT (2023) Assessment of the integrated coastal vulnerability index of Ghana toward future coastal infrastructure investment plans. Ocean Coast Manag 244:106804. https://doi.org/10.1016/j.ocecoaman.2023.106804

Chen J, Yang S, Li H, Zhang B, Lv J (2013) Research on geographical environment unit division based on the method of natural breaks (Jenks). Int Arch Photogramm Remote Sens Spatial Inf Sci 3:47–50. https://doi.org/10.5194/isprsarchives-xl-4-w3-47-2013

Dada OA, Almar R, Morand P (2024) Coastal vulnerability assessment of the West African coast to flooding and erosion. Sci Rep 14:890. https://doi.org/10.1038/s41598-023-48612-5

Davies WTR (2012) Applying a Coastal Vulnerability Index (CVI) to the Westfjords, Iceland: a preliminary assessment. University of Akureyi (MSc Thesis)

De La Cruz CPM (2021) The knowledge status of coastal and marine ecosystem services challenges, limitations and lessons learned from the application of the ecosystem services approach in management. Front Mar Sci 8:684770. https://doi.org/10.3389/fmars.2021.684770

Diez PG, Perillo GME, Piccolo MC (2007) Vulnerability to sea-level rise on the coast of the Buenos Aires Province. J Coast Res 23:119–142

Duriyapong F, Nakhapakorn K (2011) Coastal vulnerability assessment: a case study of Samut Sakhon coastal zone. Songklanakarin J Sci Technol 33:469–476

Gaki-Papanastassiou K, Karymbalis E, Poulos SE, Seni A, Zouva C (2010) Coastal vulnerability assessment to sea-level rise based on geomorphological and oceanographical parameters: the case of Argolikos Gulf, Peloponnese, Greece. Hellenic J Geosci 45:109–121

Gornitz VM (1990) Vulnerability of the East coast, U.S.A. to future sea level rise. J Coast Res 9(Suppl):201–237

Gornitz VM, Daniels RC, White TW, Birdwell KR (1994) The development of a coastal risk assessment database: vulnerability to sea-level rise in the U.S. southeast. J Coast Res 12(Suppl):327–338

Gornitz VM, Beaty TW, Daniels RC (1997) A Coastal Hazard Data Base for the U.S. West Coast. Oak Ridge National Laboratory, Oak Ridge, p 162

Gorokhovich Y, Leiserowitz A, Dugan D (2014) Integrating coastal vulnerability and community-based subsistence resource mapping in Northwest Alaska. J Coast Res 293:158–169

Hebib T, Mahdi H (2019) Estimating trends of the Mediterranean Sea level changes from tide gauge and satellite altimetry data (1993–2015). J Oceanol Limnol 37:1176–1185

Hegde AV, Reju VR (2007) Development of coastal vulnerability index for Mangalore coast, India. J Coast Res 23:1106–1111

Himmelstoss EA, Henderson RE, Kratzmann MG, Farris AS (2018) Digital shoreline analysis system (DSAS) version 5.0 user guide. In: US geological survey open file report 2018–1179

Hughes P, Brundrit GB (1992) An index to assess South Africa's vulnerability to sea-level rise. S Afr J Sci 88:308–311

IPCC (2014) Climate change 2014: synthesis report. Contribution of working groups I, II and III to the fifth assessment report of the intergovernmental panel on climate change. IPCC, Geneva, p 151 (Core Writing Team, R.K. Pachauri and L.A. Meyer (eds.))

IPCC (2019) Intergovernmental panel on climate change special report: the ocean and cryosphere in a changing climate. IPCC, Geneva

Karymbalis E, Chalkias C, Chalkias G, Grigoropoulou E, Manthos G, Ferentinou M (2012) Assessment of the sensitivity of the southern coast of the Gulf of Corinth (Peloponnese, Greece) to sea-level rise. Cent Eur J Geosci 4:561–577

Koroglu A, Ranasinghe R, Jiménez J, Ali D (2019) Comparison of coastal vulnerability index applications for Barcelona province. Ocean Coast Manag 178:104799. https://doi.org/10.1016/j.ocecoaman.2019.05.001

Kuleli T (2010) City-based risk assessment of sea level rise using topographic and census data for the Turkish coastal zone. Estuaries Coasts 33:640–651. https://doi.org/10.1007/s12237-009-9248-7

Kuleli T, Bayazıt Ş (2023) Site analysis of maritime transportation infrastructures by using the Coastal Vulnerability Index approach: The case of Bodrum Peninsula. Mar Sci Technol Bull 12(2):142–155. https://doi.org/10.33714/masteb.1260897

Kunte DP, Jauhari N, Mehrotra U, Kotha M, Hursthouse AS, Gagnon AS (2014) Multi-hazards coastal vulnerability assessment of Goa, India, using geospatial techniques. Ocean Coast Manag 95:264–281

Kurt S, Li X (2020) Potential impacts of sea level rise on the coasts of Turkey. J Env Earth Sci. https://doi.org/10.7176/JEES/10-5-04

Leatherman SP, Clow JB (1983) UMD shoreline mapping project. IEE Geosci Remote Sens Soc Newsl 22:5–8

Maanan M, Rueff H, Adouk N, Zourarah B, Rhinane H (2018) Assess the human and environmental vulnerability for coastal hazard by using a multi-criteria decision analysis. Hum Ecol Risk Assess Int J 24:1642–1658

Marcos M, Jorda G, Le Cozannet Gonéri (2016) Sub-chapter 2.2.1. Sea level rise and its impacts on the Mediterranean. In: The Mediterranean region under climate change: a scientific update. IRD Éditions, Marseille https://doi.org/10.4000/books.irdeditions.23454

Mather AA, Stretch DD, Garland GG (2010) Wave runup on natural beaches. International Conference on Coastal Engineering, Shanghai

McLaughlin S, Cooper JAG (2010) A multi-scale coastal vulnerability index: a tool for coastal managers? Environ Hazards 9(3):233–248. https://doi.org/10.3763/ehaz.2010.0052

McLaughlin S, McKenna J, Cooper JAG (2002) Socio-economic data in coastal vulnerability indices: constraints and opportunities. J Coast Res 36:487–497

Med EC (2020) Climate and Environmental Change in the Mediterranean Basin—Current Situation and Risks for the Future. Union for the Mediterranean, Plan Bleu, UNEP/MAP, Marseille https://doi.org/10.5281/zenodo.7224821. ISBN 978-2-9577416-0-1 (Cramer, W., Guiot, J., Marini, K. (eds.). 632 pp)

Mendoza ET, Salameh E, Sakho I, Turki I, Almar R, Ojeda E, Laignel B (2023) Coastal flood vulnerability assessment, a satellite remote sensing and modeling approach. Remote Sens Appl Soc Environ 29:100923

Nageswara Rao K, Subraelu P, Venkateswara Rao T, Hema Malini B, Ratheesh R, Bhattacharya S, Rajawat AS, Ajai (2008) Sea-level rise and coastal vulnerability: an assessment of Andhra Pradesh coast India through remote sensing and GIS. J Coast Conserv 12:195–207

Nicholls RJ, Cazenave A (2010) Sea-level rise and its impact on coastal zones. Science 328:1517–1520. https://doi.org/10.1126/science.1185782

OC (2017) The Ocean Conference Factsheet: People and Oceans. Ocean Conference New York 5–9 June 2017. https://sustainabledevelopment.un.org/content/documents/Ocean_Factsheet_People.pdf

Ozsahin E, Ozdes M, Ozturk M, Yang D (2023) Coastal vulnerability assessment of Thrace peninsula: implications for climate change and sea level rise. Remote Sens 15(23):5592. https://doi.org/10.3390/rs15235592

Ozyurt G, Ergin A (2010) Improving coastal vulnerability assessments to sea-level rise: a new indicator-based methodology for decision makers. J Coast Res 26:265–273

Palmer BJ, Van der Elst R, Mackay F, Mather AA, Smith AM, Bundy SC, Thackeray Z, Leuci R, Parak O (2011) Preliminary coastal vulnerability assessment for KwaZulu-Natal, South Africa. J Coast Res 64:1390–1395

Randone M, Di Carlo G, Costantini M (2017) Reviving the economy of the mediterranean sea: actions for a sustainable future. WWF Mediterranean Marine Initiative, Rome, p 64

Report EC (2016) Annex to the guide on EU funding for the tourism sector additional examples for coastal and maritime tourism. Directorate-General Maritime Affairs and Fisheries, Directorate-General Internal Market, Industry, Entrepreneurship and SMEs. ISBN 978-92-79-58873-0.

Sılaydın Aydın MB, Kahraman ED (2016) Determining the spatial vulnerability levels and Typologies of coastal cities to climate change: case of Turkey https://doi.org/10.5281/zenodo.1128163

Simav Ö, Şeker DZ, Gazioğlu C (2013) Coastal inundation due to sea level rise and extreme sea state and its potential impacts: Çukurova Delta case. Turk J Earth Sci 22(4):11

Szlafsztein C, Sterr H (2007) A GIS-based vulnerability assessment of coastal natural hazards, state of Pará, Brazil. J Coast Conserv 11:53–66

Tanim AH, Goharian E (2023) Toward an integrated probabilistic coastal vulnerability assessment: a novel copula-based vulnerability index. Water Resour Res. https://doi.org/10.1029/2022WR033603

Tanim AH, Goharian E, Moradkhani H (2022) Integrated socio-environmental vulnerability assessment of coastal hazards using data-driven and multi-criteria analysis approaches. Sci Rep 11625(2022):12. https://doi.org/10.1038/s41598-022-15237-z

Thieler ER, Hammar-Klose ES (1999) National assessment of coastal vulnerability to sea-level rise, U.S. Atlantic coast. U.S. Geological Survey, Open File Report, pp 99–593

Thieler ER, Himmelstoss EA, Zichichi JL, Ergul A (2009) The digital shoreline analysis system (DSAS) version 4.0-an arcGIS extension for calculating shoreline change (no. 2008-1278). US Geological Survey

Turkish Statistical Institute (2018) Citrus production distribution by provinces. Plant production stat. database. https://biruni.tuik.gov.tr/medas/?kn=92&locale=tr

Turkish Statistical Institute (2019) Population distribution by provinces. Address Based Pop. Sys. Database. https://biruni.tuik.gov.tr/medas/?kn=95&locale=tr

Turkish Statistical Institute (2022) Population distribution of Turkey. GIS portal of Ministry and Urbanization of Republic of Turkey

WOR (World Ocean Review) (2017) Coasts—A Vital Habitat Under Pressure. Chapter 1 Coastal Dynamics. World Ocean Rev 5:12–13 (https://worldoceanreview.com/wp-content/downloads/wor5/WOR5_en.pdf)

Yahia Meddah R, Ghodbani T, Senouci R, Rabehi W, Duarte L, Teodoro AC (2023) Estimation of the coastal vulnerability index using multi-criteria decision making: the coastal social-ecological system of Rachgoun, western Algeria. Sustainability 15(17):12838. https://doi.org/10.3390/su151712838

Yan K, Muis S, Irazoqui M, Verlaan M (2020) Water level change indicators for the European coast from 1977 to 2100 derived from climate projections. Copernicus Climate Change Service (C3S) Climate Data Store (CDS) https://doi.org/10.24381/cds.b6473cc1

Yin J, Yin Z, Wang J, Xu S (2012) National assessment of coastal vulnerability to sea-level rise for the Chinese coast. J Coast Conserv 16:123–133